analytical chemistry

pubs.acs.org/ac

Article

Heavy Metal-Induced Assembly of DNA Network Biosensor from Double-Loop Hairpin Probes for Ultrasensitive Detection of UO_2^{2+} in Water and Soil Samples

Junhua Chen,* Xu Wang, Junhui Guo, Yiwen Lv, Manjia Chen, Hui Tong, and Chengshuai Liu*

Cite This: *Anal. Chem.* 2024, 96, 3153−3159

Read Online

ACCESS | Metrics & More | Article Recommendations | Supporting Information

ABSTRACT: The uranyl ion (UO_2^{2+}) is the most stable form of uranium, which exhibits high toxicity and bioavailability posing a severe risk to human health. The construction of ultrasensitive, reliable, and robust sensing techniques for UO_2^{2+} detection in water and soil samples remains a challenge. Herein, a DNA network biosensor was fabricated for UO_2^{2+} detection using DNAzyme as the heavy metal recognition element and double-loop hairpin probes as DNA assembly materials. UO_2^{2+}-activated specific cleavage of the DNAzyme will liberate the triggered DNA fragment, which can be utilized to launch a double-loop hairpin probe assembly among H_{ab}, H_{bc}, and H_{ca}. Through multiple cyclic cross-hybridization reactions, hexagonal DNA duplex nanostructures ($n[H_{ab}\bullet H_{bc}\bullet H_{ca}]$) were formed. This DNA network sensing system generates a high fluorescence response for UO_2^{2+} monitoring. The biosensor is ultrasensitive, with a detection limit of 2 pM. This sensing system also displays an excellent selectivity and robustness, enabling the DNA network biosensor to work even in complex water and soil samples with excellent accuracy and reliability. With the advantages of enzyme-free operation, outstanding specificity, and high sensitivity, our proposed DNA network biosensor provides a reliable, simple, and robust method for trace levels of UO_2^{2+} detection in environmental samples.

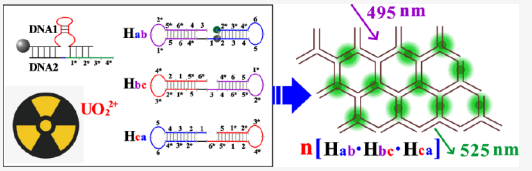

INTRODUCTION

Uranium pollution has become a serious environmental concern due to the increased release of considerable amounts of uranium into the soil and water resources through uranium mining, improper disposal of nuclear waste, and possible nuclear leakage.[1,2] Uranium with high radioactivity, chemotoxicity, and long half-life can cause acute toxicological effects and disturb the normal physiological function of kidney, brain, heart, and other organ systems.[3] Uranium possesses several forms under different conditions and the uranyl ion (UO_2^{2+}) is the most stable chemical form in water and soil samples,[4] which exhibits high bioavailability and poses severe harm to ecological system and human health.[5] With the development of nuclear mines, nuclear facilities, and nuclear weapons, an increasing amount of the radioactive wastes containing uranium is being discharged into the environment.[6] Thus, the design of sensitive and reliable detection techniques for UO_2^{2+} monitoring is of prime importance.

In recent years, some elegant detectors have been developed for UO_2^{2+} detection using organic ionophores,[7,8] peptides,[9,10] proteins,[6,11] microorganisms,[12] and nanomaterials[13,14] as recognition elements. Although these methods have made significant contributions to UO_2^{2+} detection, their selectivity remains a great challenge in sensing assays.[15] Since Lu's group reported a specific deoxyribozyme (DNAzyme) for UO_2^{2+} recognition, the selectivity for UO_2^{2+} detection has been greatly improved.[16] UO_2^{2+}−DNAzymes are a class of functional nucleic acids with catalytic properties, which display high affinity and specificity toward UO_2^{2+} binding.[17,18] Some DNAzyme-based electrochemical, fluorescent, and colorimetric biosensors have been developed for the specific detection of UO_2^{2+}.[19−21] For example, Yang et al. designed DNAzyme-grafted hydrogel for UO_2^{2+} detection and the visual detection limit was 100 nM.[22] Li and coworkers described a litmus test for UO_2^{2+} detection using DNAzyme as the recognition element and the detection limit was 65 nM.[23] Zhao et al. reported a resonance light scattering method for UO_2^{2+} assay based on the conformation change of the DNAzyme probe and the detection limit was 6.7 nM.[24] In these biosensors, their sensitivity with the nanomolar level is still not high enough for the direct detection of trace UO_2^{2+} in water and soil samples. Due to the strong radioactivity and enrichment characteristics, ultratrace UO_2^{2+} in real samples can also pose a threat to human health. Therefore, it is highly desirable and interesting to develop an ultrasensitive biosensor for UO_2^{2+} detection with excellent specificity and reliability.

Signal amplification is an efficient way to improve the detection sensitivity in biosensor design.[25] The commonly used protein enzyme-mediated signal amplification strategies

Received: December 5, 2023
Revised: January 22, 2024
Accepted: January 26, 2024
Published: February 6, 2024

https://doi.org/10.1021/acs.analchem.3c05526
Anal. Chem. 2024, 96, 3153−3159

Scheme 1. Detection Mechanism of the DNA Network Biosensor for the Ultrasensitive Detection of UO_2^{2+} Based on Double-Loop Hairpin Probes Assembly[a]

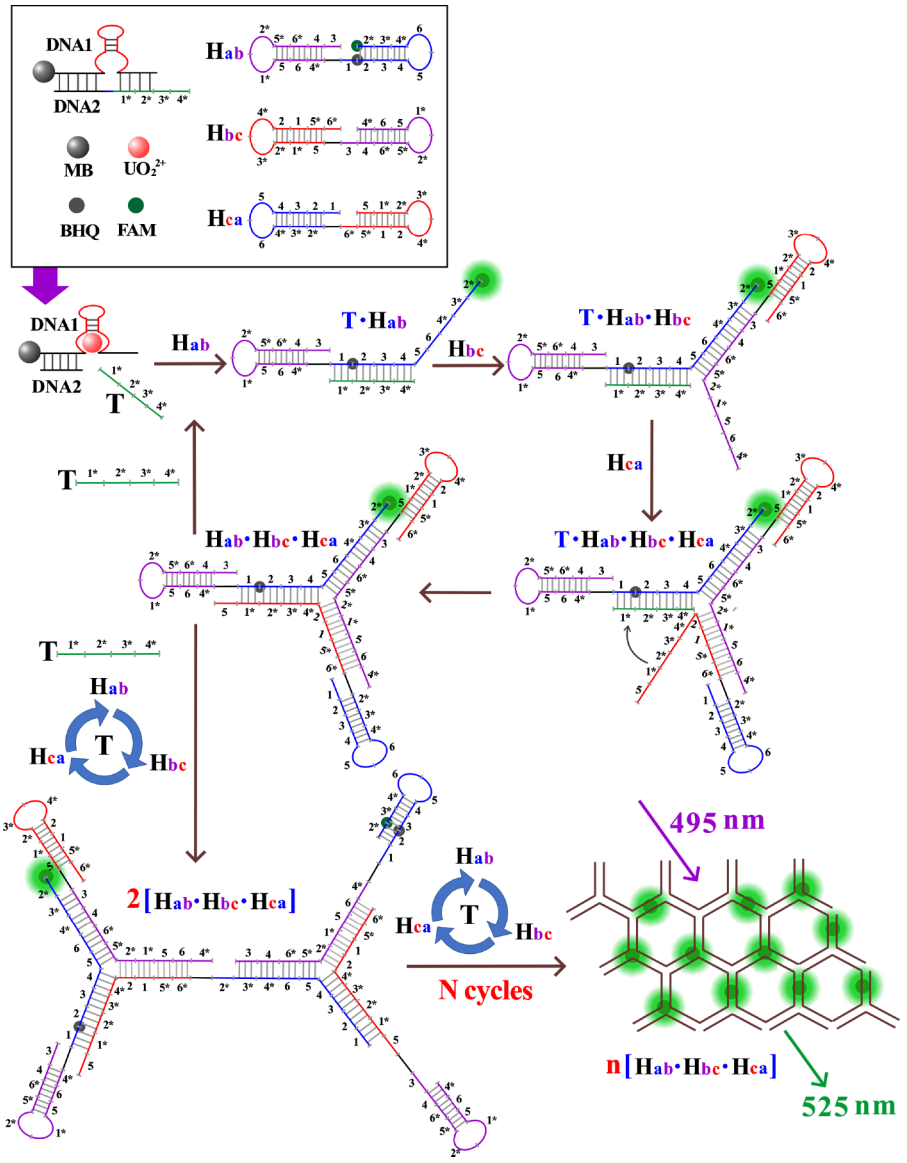

[a]UO_2^{2+}-specific DNAzyme (DNA1 and DNA2) was used to identify UO_2^{2+}. Double-loop hairpin probes (H_{ab}, H_{bc}, and H_{ca}) were utilized to build the DNA network. DNA1 was immobilized on magnetic beads (MB). H_{ab} was modified with FAM and BHQ.

have received great attention in biosensor fabrication using horseradish peroxidase,[26] phosphatase,[27] exonuclease,[28] and polymerase[29] as catalysts. However, the enzyme is costly and susceptible to environmental factors, such as temperature and pH.[30] Moreover, heavy metals can significantly reduce the catalytic activity of proteases.[31,32] Thus, there is an urgent need to develop an enzyme-free signal amplification approach for trace heavy metal detection in complex matrix samples. As an ideal alternative, signal amplification originating from DNA assembly can provide an enzyme-free format for target assay with high sensitivity.[33−35] With the advantages of high stability and flexibility, simple operation procedure, low cost, and convenient scalability, DNA assembly has been used in environmental monitoring and clinical diagnosis.[36−38] Exploring the construction of novel DNA assembly methods and applying them to the ultrasensitive detection of heavy metals is an interesting and challenging task.

Herein, a DNA network biosensor was developed for the ultrasensitive detection of UO_2^{2+} on the basis of double-loop hairpin probes assembly. Through multiple cyclic cross-hybridization reactions, the DNA network sensing system containing some hexagonal DNA nanostructures ($n[H_{ab}\bullet H_{bc}\bullet H_{ca}]$) will be obtained to produce a high fluorescence signal for heavy metal detection. The biosensor has a high sensitivity, with a detection limit of 2 pM. With excellent accuracy and reliability, the robust DNA network biosensor can be employed for UO_2^{2+} detection in water and soil samples.

EXPERIMENTAL SECTION

Materials. DNA probes used in this work are shown in Table S1. The sequences were synthesized by Sangon Biotech Co., Ltd. (Shanghai, China). Magnetic beads (MB) of 1 μM in diameter coated with streptavidin (SA) were obtained from

https://doi.org/10.1021/acs.analchem.3c05526
Anal. Chem. 2024, 96, 3153−3159

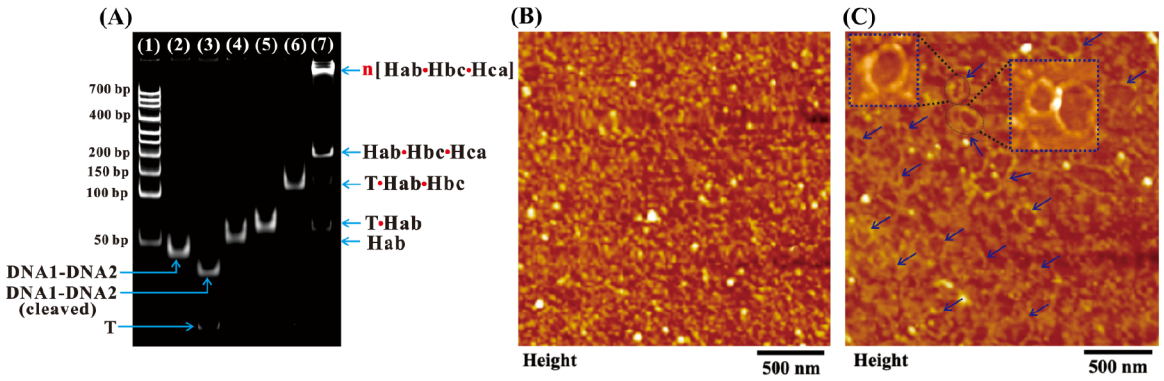

Figure 1. (A) PAGE characterization of the DNA network assembly strategy. Lane 1: DNA marker. Lane 2: DNA1 + DNA2. Lane 3: UO_2^{2+} + DNA1 + DNA2. Lane 4: H_{ab}. Lane 5: T + H_{ab}. Lane 6: T + H_{ab} + H_{bc}. Lane 7: T + H_{ab} + H_{bc} + H_{ca}. (B) AFM image of the DNA mixture in the absence of UO_2^{2+}. (C) AFM image of the DNA network (hexagonal nanostructure) in the presence of UO_2^{2+}. Inset shows a magnified view of the outlined structure.

Aladdin Biochemical Technology Co., Ltd. (Shanghai, China). All commercially obtained chemicals were of analytically pure grade. All buffers were prepared with Milli-Q water (18.2 MΩ/cm).

Procedures for UO_2^{2+} Detection. The working buffer is a 50 mM MES buffer solution (pH 6.5) containing 150 mM $NaNO_3$. All DNA probes were separately dissolved in the working buffer, heated at 98 °C for 10 min, and then slowly cooled to room temperature. 100 nM biotinylated DNA1 was incubated with SA-MB solution (100 μL, 1.5 mg/mL) for 20 min. After magnetic separation, MB-DNA1 was redispersed in the working buffer. 150 nM DNA2 was then incubated with MB-DNA1 for 20 min. After magnetic separation, the obtained MB-DNA1−DNA2 complex were dispersed in the working buffer. Then, the target UO_2^{2+} was added to the above mixture, and the mixture was incubated for 40 min. The supernatant after magnetic separation was added to a solution of 200 nM H_{ab}, H_{bc}, and $H_{c.}$ After incubation for 60 min, a SpectraMax i3x (Molecular Devices, San Jose, USA) was used to record the fluorescence signals.

Real Sample Assay. The seawater was collected from the east coast of Zhuhai City, Guangdong Province, China. The seawater was filtered using a 0.22 μm filter membrane to remove the marine microorganisms and suspended particles. After 10-fold dilution with the working buffer, seawater was detected using our proposed biosensor. The soil samples were collected near uranium mines in Nanxiong City, Guangdong Province, China. After thoroughly grinding, the soil samples were sieved with a 0.15 mm mesh. 0.2 g soil was mixed with 10 mL HNO_3 and incubated at room temperature for 1 h. The pH of the soil solution was adjusted to 6.5 with 1 M NaOH and then filtered through a 0.22 μm filter membrane. After 50-fold dilution using the working buffer, the soil samples were detected by using our proposed biosensor. The traditional ICP−MS method was also used to verify the detection results of the DNA network biosensor.

Atomic Force Microscopy (AFM) Characterization. 5 μL of $NiCl_2$ (5 mM) was dropped onto the freshly cleaved silicon wafer and incubated for about 3 min. 10 μL of diluted DNA reaction products was deposited onto the treated silicon wafer for 5 min. Samples were then rinsed with deionized water for three times and dried at room temperature. AFM experiments were carried out in ambient air under the tapping mode on a Multimode 8 instrument (Bruker, Germany).

Native Polyacrylamide Gel Electrophoresis (PAGE). The operational procedures of the native PAGE are described in the Supporting Information.

RESULTS AND DISCUSSION

Detection Mechanism. The detection mechanism of the DNA network biosensor for the ultrasensitive detection of UO_2^{2+} is illustrated in Scheme 1. UO_2^{2+}-specific DNAzyme (DNA1 and DNA2) was used as the heavy metal recognition element. The enzyme strand DNA1 was immobilized on MB and the substrate strand DNA2 contained the trigger strand of 1*−2*−3*−4*. The assembly probes contained three double-loop hairpin DNA (H_{ab}, H_{bc}, and H_{ca}), in which H_{ab} is modified with the fluorophore (FAM) and the quencher (BHQ). In the presence of UO_2^{2+}, DNA2 will be cleaved into two parts, and the blocked trigger strand (T, 1*−2*−3*−4*) is liberated. After magnetic separation, the free T can activate the assembly reactions among the hairpin probes. MB was used to immobilize DNA1−DNA2 complex that can minimize unwanted crosstalk (leak) reactions. Using domain 1* as a toehold, T can open H_{ab} through a toehold-mediated stand displacement reaction (domain hybridization between 1*−2*−3*−4* and 1−2−3−4). In the formed T•H_{ab} intermediate, newly opened domain 3* can further hybridize to domain 3 of H_{bc}, again activating a toehold reaction (DNA hybridization between 3*−4*−6−5 and 3−4−6*-5*) to open H_{bc} and generate the T•H_{ab}•H_{bc} complex, in which segment 6 is no longer occluded. Similarly, segment 6 can bind to segment 6* of H_{ca} and then open H_{ca} through toehold-mediated stand displacement to generate the T•H_{ab}•H_{bc}•H_{ca} hybrid. Then, T will spontaneously dissociate, and the stable H_{ab}•H_{bc}•H_{ca} complex will be formed. The released T can be recycled to activate other assembly reactions in H_{ab}, H_{bc}, and H_{ca}. Importantly, as each of the hairpin probes contains the double-loop structure, the H_{ab}•H_{bc}•H_{ca} complex can further hybridize to H_{ab}, H_{bc}, and H_{ca}. Through multiple cyclic cross-hybridization reactions, the DNA network (n[H_{ab}•H_{bc}•H_{ca}]) that contains some DNA hexagon nanostructures will be formed. The separation of FAM and BHQ in the network sensing system generates a high fluorescence intensity for UO_2^{2+} detection. If there is no UO_2^{2+} in the solution, then domain 1* in T will be blocked. The inaccessible T failed to trigger toehold binding among H_{ab}, H_{bc}, and H_{ca}. And only a

https://doi.org/10.1021/acs.analchem.3c05526
Anal. Chem. 2024, 96, 3153−3159

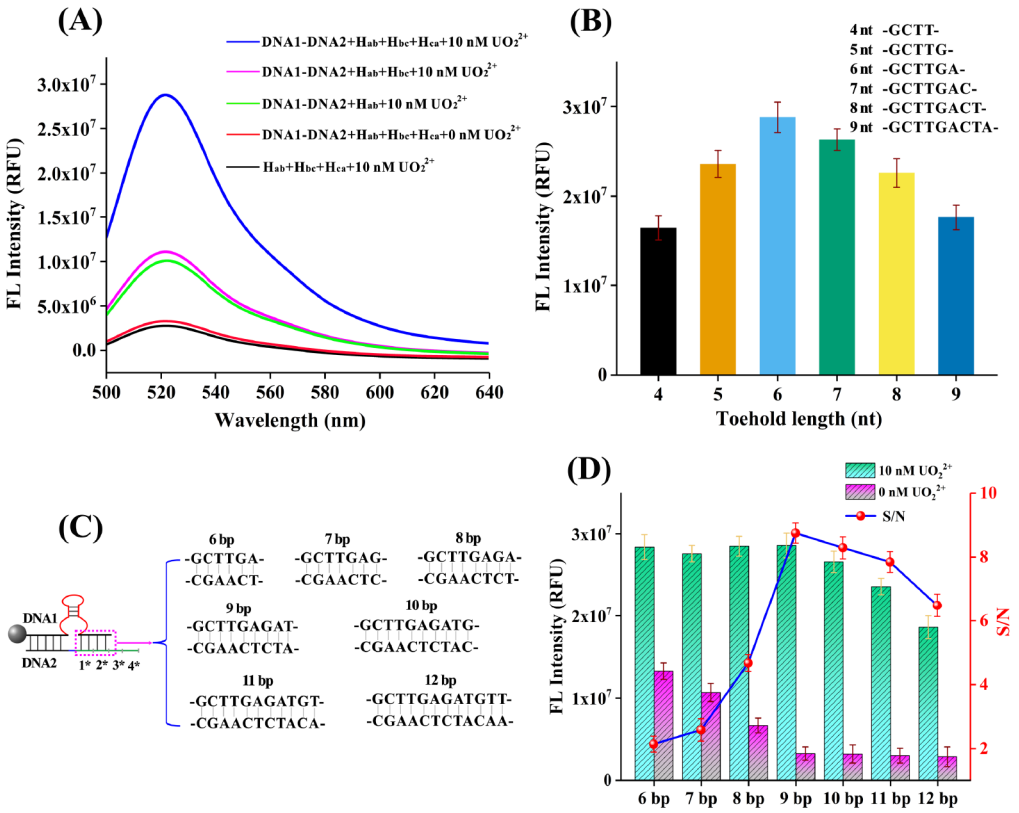

Figure 2. (A) Fluorescence responses of the DNA network biosensor to different reaction combinations. (B) Effect of toehold lengths (domain 1 in H_{ab}) on the fluorescence responses of the DNA network biosensor. (C) Complementary base pairs (from 6 to 12 bp) between T and the right arm of DNA1. (D) Effect of complementary base pair lengths (between T and the right arm of DNA1) on the fluorescence intensity of the DNA network biosensor.

weak background fluorescence response can be obtained for the blank sample.

PAGE and AFM Characterization. The native PAGE experiments were executed to demonstrate the cleavage process between UO_2^{2+} and DNA1−DNA2 and the assembly reactions among H_{ab}, H_{bc}, and H_{ca}. As shown in Figure 1A, the bands in lane 1 are the DNA marker. The band in lane 2 is the DNA1−DNA2 duplex. When incubating UO_2^{2+} with DNA1−DNA2, we can observe two bands in lane 3, which originated from the cleaved DNA1−DNA2 and the released T strand, respectively. Such PAGE results indicated that UO_2^{2+} can cleave UO_2^{2+}-specific DNAzyme (DNA1−DNA2) and that the trigger strand (T) was indeed released. The band in lane 4 is H_{ab}. When H_{ab} is mixed with T, the T•H_{ab} intermediate can be obtained in lane 5, implying that the trigger strand T can open H_{ab}. In the presence of T, H_{ab}, and H_{bc}, we can observe assembled product T•H_{ab}•H_{bc} in lane 6. After mixing T, H_{ab}, H_{bc}, and H_{ca}, a bright band with significantly reduced mobility can be clearly observed in lane 7, which represented the assembled DNA network product (n[H_{ab}•H_{bc}•H_{ca}]). The other bands in lane 7 correspond to the redundant intermediates. These PAGE results successfully verified the assembly process among double-loop hairpin probes, and the DNA network was formed in the sensing system. Besides, the morphology of the formed DNA network was characterized by AFM. As shown in Figure 1B,C, the DNA network structure containing some similar hexagon DNA (marked by green arrows) appeared as anticipated upon the addition of UO_2^{2+} to the sensing system. The inset of Figure 1C shows a magnified view of the outlined hexagonal DNA nanostructure. The AFM results further confirmed the successful assembly of the DNA network sensing system.

Fluorescence Response Characterization. The fluorescence response characteristics of the DNA network sensing system for UO_2^{2+} detection were further verified under different conditions. As shown in Figure 2A, the solution of H_{ab}, H_{bc}, and H_{ca} had a weak fluorescence response even after incubation with 10 nM UO_2^{2+} (black curve), indicating that double-loop hairpin probes are stable and can coexist in solution. The DNA1−DNA2, H_{ab}, H_{bc}, and H_{ca} solution also showed a weak fluorescence signal (red curve) because no cleave reaction occurred in the absence of UO_2^{2+} and the trigger strand (T, 1*−2*−3*−4*) was still blocked. Both the solution of DNA1−DNA2 + H_{ab} + 10 nM UO_2^{2+} and DNA1−DNA2 + H_{ab} + H_{bc} + 10 nM UO_2^{2+} showed slight fluorescence recovery (green and pink curves). UO_2^{2+} can cleave DNA1−DNA2 and release T, which will open H_{ab} and H_{bc} to form the T•H_{ab} and T•H_{ab}•H_{bc} complex. The separation of FAM and BHQ in these complexes thus generates the fluorescence signals. In the presence of DNA1−DNA2, H_{ab}, H_{bc}, H_{ca}, and UO_2^{2+}, the fluorescence signal was significantly enhanced (blue curve), implying that UO_2^{2+} can activate the cyclic assemblies of the double-loop hairpin probes to continuously produce the DNA network products. These results indicated that the double-loop hairpin probe-mediated formation of a DNA network can be used for the ultrasensitive detection of UO_2^{2+}.

The hairpin assembly reaction is based on the toehold-mediated stand displacement. Domain 1 in H_{ab} serves as the toehold domain to initiate the strand replacement reaction for the assembly of double-loop hairpins. The assembly efficiency

https://doi.org/10.1021/acs.analchem.3c05526
Anal. Chem. 2024, 96, 3153−3159

is affected by the length of domain 1. As the base number in domain 1 increased from 4 to 6 nt, the fluorescence signal gradually increased and reached its highest value at 6 nt (Figure 2B). Further increasing the base number resulted in a decrease in the fluorescence signal. In the toehold-mediated displacement reaction, the hybridization of toeholds should be strong enough to ensure the occurrence of strand replacement reactions. At the same time, such hybridization should be weak enough to ensure toehold liberation for reuse. Thus, the optimal base number of the toehold domain was set as 6 nt.

In the presence of UO_2^{2+}, DNA1−DNA2 will be cut into two parts, and the liberated T (1*−2*−3*−4*) can be used to activate the hairpin assembly. The length of the complementary base pair between T and the right arm of DNA1 will determine whether T can be released. As shown in Figure 2C, different complementary base pairs (from 6 to 12 bp) were designed to investigate the optimal length. With the increase in the base pairs from 6 to 9 bp, the fluorescence response in the presence of UO_2^{2+} almost remained stable and started to decrease when the base pairs exceeded 9 bp. Excessive complementary base pairs will cause difficulty in releasing the T strand. We can also observe that the background signal was maintained in a high value when the base pairs are less than 9 bp. Insufficient complementary base pairs will cause a high noise. Thus, to achieve the best signal-to-noise (S/N) ratio (blue line), 9 bp complementary base pairs between T and the right arm of DNA1 were used in the sensing system.

Comparison of Single- and Double-Loop Hairpin Assemblies. Conventional hairpin assembly requires only single-loop hairpin probes to complete the assembly reaction. As shown in Figure 3A, single-loop hairpin probes H_a, H_b, and H_c can assemble into the single Y-shaped DNA structure (H_a•H_b•H_c) for UO_2^{2+} detection (the assembly process is shown in Scheme S1). In the double-loop hairpin probe assembly (Figure 3B), the DNA network (n[H_{ab}•H_{bc}•H_{ca}]) containing some hexagon DNA duplex structures will be formed. Figure 3C is the real-time fluorescence responses of the single- and double-loop hairpin probe assemblies for UO_2^{2+} detection. Without UO_2^{2+} in the sensing system, both the single- and double-loop hairpin assemblies had weak background signals. With UO_2^{2+} in the sensing system, the response signal of the single-loop hairpin assembly slowly increased with the gradual extension of the incubation time. The single-loop hairpin assembly takes 100 min to reach equilibrium. In the double-loop hairpin assembly, with an increase in the reaction time, the fluorescence response increased sharply. An equilibrium value of the response signal can be obtained after 60 min. Compared with the single-loop hairpin assembly, the double-loop hairpin assembly has a higher detection sensitivity due to the less reaction time and more efficient signal amplification capability.

Analytical Performance for UO_2^{2+} Detection. To get the best analytical results for UO_2^{2+} sensing, several experimental parameters (the hairpin concentration, the reaction temperature, the salt concentration, and the pH of the working buffer) were systematically optimized (Figures S1−S4). Under optimal assay conditions, different concentrations of UO_2^{2+} were tested by the DNA network biosensor. As shown in Figure 4A, with an increase in UO_2^{2+} concentrations from 0 to 5 μM, the fluorescence response gradually increased. Figure 4B shows the calibration curve of fluorescence responses at 525 nm over concentrations of UO_2^{2+}. The linear range for UO_2^{2+} detection is from 10 pM to

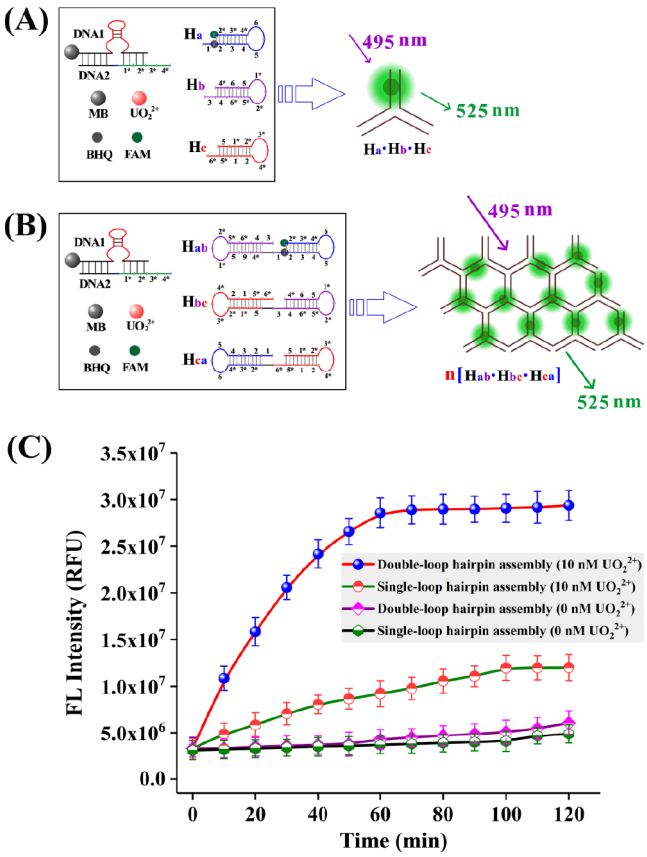

Figure 3. (A) Single-loop hairpin probes assembly strategy for UO_2^{2+} sensing. (B) Double-loop hairpin probes assembly strategy for UO_2^{2+} sensing. (C) Fluorescence signals for single- and double-loop hairpin probes assembly for UO_2^{2+} detection.

1 μM. The regression equation is $F = 6.53 \times 10^6$ Lg $C + 1.33 \times 10^6$ ($R^2 = 0.992$), where F and C are the fluorescence signal and UO_2^{2+} concentration, respectively. The detection limit of this DNA network biosensor was calculated to be 2 pM (S/N = 3). Compared to previously reported UO_2^{2+} sensors (Table S2), our constructed DNA network biosensor displayed superior detection sensitivity. Such high sensitivity should be ascribed to the efficient signal amplification capability of the DNA network sensing system, which can generate hexagon DNA nanostructures (n[H_{ab}•H_{bc}•H_{ca}]) with improved fluorescence signals.

Selectivity Investigation. To evaluate the selectivity of the DNA network sensing system for the UO_2^{2+} assay, several other heavy metal ions (Pb^{2+}, Cd^{2+}, Hg^{2+}, Cu^{2+}, As^{3+}, Fe^{2+}, and Cr^{3+}) were tested. As shown in Figure 5, the nontarget heavy metals and the control mixture at 1 or 100 nM did not cause significant fluorescence signal changes compared with the blank test. Only the target UO_2^{2+} generates a strong fluorescence response. In addition, adding UO_2^{2+} to the mixture of the control heavy metal ions can also generate a strong fluorescence signal. The above results indicated that the DNA network biosensor has good selectivity, which is beneficial for UO_2^{2+} monitoring in practical samples.

Detection of Real Samples. To verify the practicality of the sensing strategy, the DNA network biosensor was hired to assay UO_2^{2+} concentrations in seawater and soil samples. The seawater samples were collected from the east coast of Zhuhai City, Guangdong Province. The soil samples were collected

https://doi.org/10.1021/acs.analchem.3c05526
Anal. Chem. 2024, 96, 3153−3159

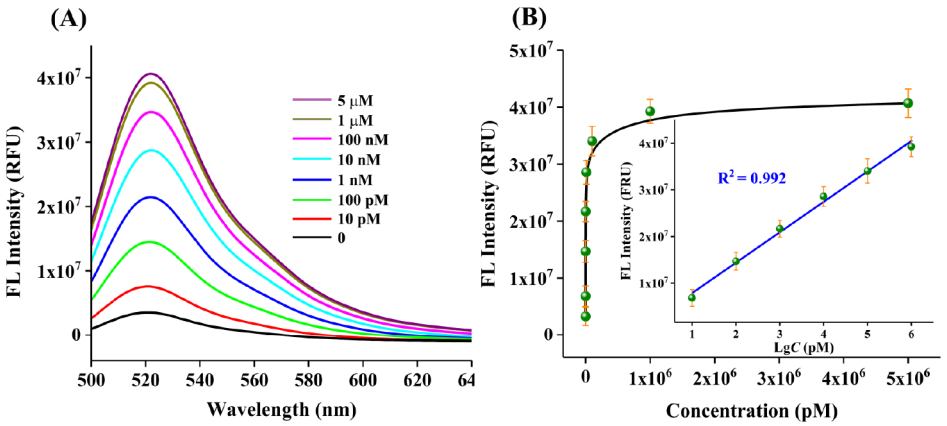

Figure 4. (A) Fluorescence spectra of the DNA network biosensor treated with different concentrations of UO_2^{2+}. (B) The calibration curve and linear range of the DNA network biosensor for UO_2^{2+} detection.

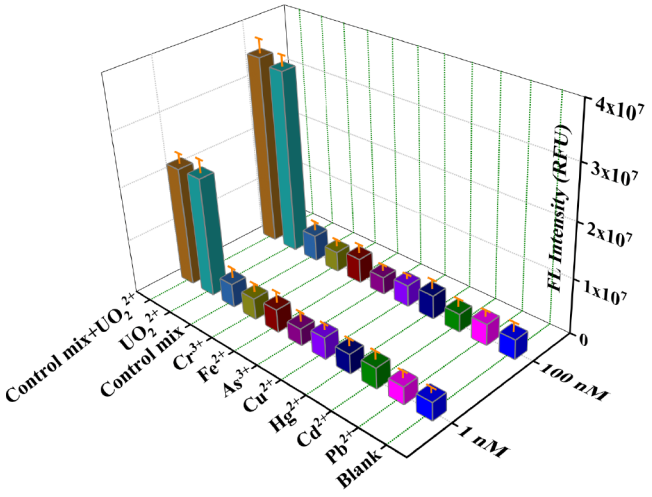

Figure 5. Selectivity of the DNA network sensing system for UO_2^{2+} and several control heavy metal ions. The concentrations of all tested substances are 1 and 100 nM.

near uranium mines in Nanxiong City, Guangdong Province. The actual samples were detected by using both the DAN network biosensor and the conventional ICP-MS technique. The data are shown in Tables S3 and S4. It can be clearly seen that the detection results of the DNA network biosensor were almost in good agreement with the conventional ICP−MS method. The DNA network biosensor has a relative standard deviation (RSD) from 2.4% to 5.2% (n = 3). The biosensor has a relative error (Re) from −5.6% to 6.3% compared with the ICP−MS method. With excellent accuracy and reliability, the robust DNA network biosensor can be used to detect the UO_2^{2+} concentration in complex samples.

CONCLUSIONS

In conclusion, we have successfully built a DNA network biosensor for the ultrasensitive detection of UO_2^{2+} using double-loop hairpin probe assembly, which is an efficient signal amplification strategy for a heavy metal assay. The UO_2^{2+}−DNAzyme interactions will free the trigger DNA fragment, which can be utilized to initiate the cyclic assemblies among the probes of H_{ab}, H_{bc}, and H_{ca}. The formed products of the DNA network ($n[H_{ab}•H_{bc}•H_{ca}]$) with hexagon nanostructures can yield an improved fluorescence response for UO_2^{2+} detection. The ($n[H_{ab}•H_{bc}•H_{ca}]$) DNA network sensing platform has not been reported before. The innovative DNA network biosensor has a wide linear range for UO_2^{2+} detection from 10 pM to 1 μM. And the biosensor is ultrasensitive, with a detection limit of 2 pM. Such outstanding sensitivity is ascribed to the multiple cyclic cross-hybridization reactions among three double-loop hairpin probes. Benefiting from the specific UO_2^{2+}−DNAzyme interactions and magnetic separation operation, the biosensor exhibits an excellent selectivity, and the interfering heavy metals do not affect the analytical performance. The proposed DNA network sensing system was used to detect UO_2^{2+} in seawater and soil samples. The biosensor is robust and the real samples test data are in good agreement with the conventional ICP−MS assay. The DNA network sensing system is an enzyme-free signal amplification model, which is beneficial for maintaining the stability of biosensor when confronted with complex matrix samples. With the advantages of excellent sensitivity and selectivity, simple operation, and user-friendliness, the DNA network biosensor can be used for UO_2^{2+} monitoring to indicate uranium pollution in water and soil samples.

ASSOCIATED CONTENT

Supporting Information

The Supporting Information is available free of charge at https://pubs.acs.org/doi/10.1021/acs.analchem.3c05526.

PAGE procedure, the supplementary tables (Tables S1−S4), and the supplementary figures (Scheme S1 and Figures S1−S4) (PDF)

AUTHOR INFORMATION

Corresponding Authors

Junhua Chen − *State Key Laboratory of Environmental Geochemistry, Institute of Geochemistry, Chinese Academy of Sciences, Guiyang 550081, China; National-Regional Joint Engineering Research Center for Soil Pollution Control and Remediation in South China, Guangdong Key Laboratory of Integrated Agro-Environmental Pollution Control and Management, Institute of Eco-Environmental and Soil Sciences, Guangdong Academy of Sciences, Guangzhou 510650, China;* orcid.org/0000-0001-9450-7272; Email: 222chenjunhua@163.com

Chengshuai Liu − *State Key Laboratory of Environmental Geochemistry, Institute of Geochemistry, Chinese Academy of*

https://doi.org/10.1021/acs.analchem.3c05526
Anal. Chem. 2024, 96, 3153−3159

Sciences, Guiyang 550081, China; orcid.org/0000-0003-0133-0119; Email: liuchengshuai@vip.gyig.ac.cn

Authors

Xu Wang − *Institute of Quality Standard and Monitoring Technology for Agro-Products, Guangdong Academy of Agricultural Sciences, Guangzhou 510640, China;* orcid.org/0000-0002-4617-0860

Junhui Guo − *School of Material and Food, Jiangmen Polytechnic, Jiangmen 529000, China*

Yiwen Lv − *National-Regional Joint Engineering Research Center for Soil Pollution Control and Remediation in South China, Guangdong Key Laboratory of Integrated Agro-Environmental Pollution Control and Management, Institute of Eco-Environmental and Soil Sciences, Guangdong Academy of Sciences, Guangzhou 510650, China*

Manjia Chen − *National-Regional Joint Engineering Research Center for Soil Pollution Control and Remediation in South China, Guangdong Key Laboratory of Integrated Agro-Environmental Pollution Control and Management, Institute of Eco-Environmental and Soil Sciences, Guangdong Academy of Sciences, Guangzhou 510650, China*

Hui Tong − *National-Regional Joint Engineering Research Center for Soil Pollution Control and Remediation in South China, Guangdong Key Laboratory of Integrated Agro-Environmental Pollution Control and Management, Institute of Eco-Environmental and Soil Sciences, Guangdong Academy of Sciences, Guangzhou 510650, China*

Complete contact information is available at: https://pubs.acs.org/10.1021/acs.analchem.3c05526

Notes

The authors declare no competing financial interest.

■ ACKNOWLEDGMENTS

This work was supported by the National Natural Science Foundations of China (42025705 and 42377454), GDAS' Project of Science and Technology Development, China (2019GDASYL-0103048), the Guangdong Provincial Agricultural Team Innovation Project (2023KJ112), and the National Key Research and Development Program of China (2020YFC1808500).

■ REFERENCES

(1) Yuan, Y.; Liu, T.; Xiao, J.; Yu, Q.; Feng, L.; Niu, B.; Feng, S.; Zhang, J.; Wang, N. *Nat. Commun.* **2020**, *11* (1), 5708.
(2) He, W.; Hua, D. *Talanta* **2019**, *201*, 317−329.
(3) Gao, N.; Huang, Z.; Liu, H.; Hou, J.; Liu, X. *Chemosphere* **2019**, *237*, 124548.
(4) Dutta, R. K.; Kumar, A. *Anal. Chem.* **2016**, *88*, 9071−9078.
(5) Yuan, Y.; Yu, Q.; Cao, M.; Feng, L.; Feng, S.; Liu, T.; Feng, T.; Yan, B.; Guo, Z.; Wang, N. *Nat. Sustain.* **2021**, *4*, 708−714.
(6) Feng, T.; Yuan, Y.; Zhao, S.; Feng, L.; Yan, B.; Cao, M.; Zhang, J.; Sun, W.; Lin, K.; Wang, N. *Angew. Chem. Int. Ed.* **2022**, *61* (10), No. e202115886.
(7) Zhang, Y.; Sun, L.; Yan, Q.; Qiu, X.; Cheng, Y.; Wang, B.; Tan, X.; Fang, M.; Luck, R. L.; Liu, H. *Microchem. J.* **2022**, *180*, 107619.
(8) Ma, J.; He, W.; Han, X.; Hua, D. *Talanta* **2017**, *168*, 10−15.
(9) Roozbahan, G. M.; Chen, X.; Zhang, Y.; Xie, R.; Ma, R.; Li, D.; Li, H.; Guan, X. *ACS Sens.* **2017**, *2*, 703−709.
(10) Yang, C.; Han, J.; Gu, M.; Liu, J.; Li, Y.; Huang, Z.; Yu, H.; Hu, S.; Wang, X. *Chem. Commun.* **2015**, *51*, 11769−11772.
(11) Arredondo, G. P.; Holt, S. A.; He, L. *Acs Appl. Nano Mater.* **2021**, *4*, 11801−11808.
(12) Cecal, A.; Humelnicu, D.; Rudic, V.; Cepoi, L.; Ganju, D.; Cojocari, A. *Bioresour. Technol.* **2012**, *118*, 19−23.
(13) Wang, D.; Zhang, L.; Liu, M.; Du, F.; Shen, Z.; He, L.; Wang, L. *J. Hazard. Mater.* **2023**, *454*, 131497.
(14) Lin, X.; Xuan, D.; Liang, H.; Xiao, F.; Li, F.; Liu, C.; Fan, P.; Hu, C.; Yang, S.; Liu, Y. *J. Environ. Radioact.* **2020**, *220*−*221*, 106299.
(15) Farzin, L.; Shamsipur, M.; Sheibani, S.; Samandari, L.; Hatami, Z. *Microchim. Acta* **2019**, *186* (5), 289.
(16) Liu, J.; Brown, A. K.; Meng, X.; Cropek, D. M.; Istok, J. D.; Watson, D. B.; Lu, Y. *Proc. Natl. Acad. Sci. U. S. A.* **2007**, *104*, 2056−2061.
(17) Brown, A. K.; Liu, J.; He, Y.; Lu, Y. *ChemBiochem* **2009**, *10*, 486−492.
(18) Feng, M.; Gu, C.; Sun, Y.; Zhang, S.; Tong, A.; Xiang, Y. *Anal. Chem.* **2019**, *91*, 6608−6615.
(19) Sun, L.; Liu, J.; Li, L.; Zhen, D.; Dai, Z.; Tang, S.; Zhu, B.; Chen, L.; Chen, H.; Gong, M.; Tang, Z.; Hu, Y. *Inorg. Chem. Commun.* **2022**, *138*, 109234.
(20) Bai, Y.; Xu, L.; Chai, H.; Zhou, L.; Jiang, G.; Zhang, G. *Front. Chem.* **2022**, *10*, 882250.
(21) Zhang, L.; Tan, Q.; Xiao, S.; Yang, G.; Liu, X.; Zheng, Q.; Fan, J.; Liang, R.; Qiu, J. *Anal. Chem.* **2023**, *95*, 4703−4711.
(22) Huang, Y.; Fang, L.; Zhu, Z.; Ma, Y.; Zhou, L.; Chen, X.; Xu, D.; Yang, C. *Biosens. Bioelectron.* **2016**, *85*, 496−502.
(23) Manochehry, S.; McConnell, E. M.; Tram, K. Q.; Macri, J.; Li, Y. *Front. Chem.* **2018**, *6*, 332.
(24) Zhou, B.; Wang, Y.; Yang, H.; Xue, J.; Wang, J.; Liu, S.; Liu, H.; Zhao, H. *Microchim. Acta* **2014**, *181*, 1353−1360.
(25) Zhu, Y.; Wu, J.; Zhou, Q. *Biosens. Bioelectron.* **2023**, *230*, 115282.
(26) Liu, L.; Xu, Z.; Vargas, A. M. M.; Dollery, S. J.; Schrlau, M. G.; Cormier, D.; O'Connell, M. R.; Tobin, G. J.; Du, K. *Anal. Chem.* **2023**, *95*, 11997−12005.
(27) Gianvittorio, S.; Gualandi, I.; Tonelli, D. *Molecules* **2023**, *28*, 1532.
(28) Zhao, X.; Yuan, Y.; Liu, X.; Mao, F.; Xu, G.; Liu, Q. *Anal. Chem.* **2022**, *94*, 2298−2304.
(29) Li, J.; Du, Z.; Wang, P.; Chen, K.; Lin, S.; Xu, W.; Zhu, L. *Anal. Chim. Acta* **2023**, *1279*, 341827.
(30) Nguyen, H. H.; Lee, S. H.; Lee, U. J.; Fermin, C. D.; Kim, M. *Materials* **2019**, *12*, 121.
(31) Guo, W.; Zhang, C.; Ma, T.; Liu, X.; Chen, Z.; Li, S.; Deng, Y. *J. Nanobiotechnol.* **2021**, *19* (1), 166.
(32) Vonnie, J. M.; Rovina, K.; Mariah, A. M. A.; Erna, K. H.; Felicia, W. X. L.; Aqilah, M. N. N. *Int. J. Environ. Sci. Technol.* **2023**, *20* (7), 8041−8072.
(33) Zhang, Y.; Chai, Y.; Wang, H.; Yuan, R. *Anal. Chem.* **2019**, *91*, 14368−14374.
(34) Cao, T.; Jia, H.; Dong, Y.; Gui, S.; Liu, D. *ACS Appl. Mater. Interfaces* **2020**, *12*, 4185−4192.
(35) Yao, C.; Ou, J.; Tang, J.; Yang, D. *Acc. Chem. Res.* **2022**, *55*, 2043−2054.
(36) Guo, Y.; Li, S.; Tong, Z.; Tang, J.; Zhang, R.; Lv, Z.; Song, N.; Yang, D.; Yao, C. *J. Am. Chem. Soc.* **2023**, *145*, 23859−23873.
(37) Wang, C.; Han, C.; Du, X.; Guo, W. *Anal. Chem.* **2021**, *93*, 12881−12888.
(38) Dong, J.; Ouyang, Y.; Wang, J.; O'Hagan, M. P.; Willner, I. *ACS Nano* **2022**, *16*, 6153−6164.